Journal of
Composites Science

MDPI

Article

Development of Doum Palm Fiber-Based Building Insulation Composites with Citric Acid/Glycerol Eco-Friendly Binder

Hicham Elmoudnia [1,*], Younoussa Millogo [2], Paulina Faria [3], Rachid Jalal [4,5], Mohamed Waqif [1] and Latifa Saâdi [1]

[1] Laboratory of Innovative Materials, Energy and Sustainable Development (IMED-Lab), Faculty of Science and Technology, Cadi Ayyad University, Marrakech 40000, Morocco
[2] Laboratoire de Chimie et Energies Renouvelables (LaCER), Unité de Formation et de Recherche en Sciences Exactes et Appliquées (UFR/SEA), Université Nazi BONI, Bobo-Dioulasso 01 BP 1091, Burkina Faso; millogokadi@gmail.com
[3] CERIS, Department of Civil Engineering, NOVA School of Science and Technology, NOVA University of Lisbon, 2829-516 Caparica, Portugal; mpr@fct.unl.pt
[4] Laboratoire de Recherche en Développement Durable et Santé (LRDDS), Faculty of Science and Technology, Cadi Ayyad University, Marrakech 40000, Morocco; r.jalal@uca.ma
[5] Centre d'Agrobiotechnologie et Bioingénierie, Unité de Recherche Labellisée CNRST (Centre AgroBiotech, URL-CNRST 05), Cadi Ayyad University, Marrakech 40000, Morocco
* Correspondence: hicham.elmoudnia@ced.uca.ma

Abstract: This study focuses on the development of an insulation biocomposite using Doum palm (Chamaerops humilis) fibers reinforced with a natural binder based on citric acid and glycerol. The main objective is to optimize the thermal conductivity and mechanical properties of the biocomposite as a function of fiber preparation (short or powdered fibers) and binder content (20%, 30% and 40%), and relate them to the bonding of the fibers and the binder. The obtained results suggest that the addition of the binder greatly enhances the density, compressive strength and Young's modulus of biocomposites. More specifically, the addition of 20% by weight of the citric acid/glycerol binder improves the bond between fibers, whether they are short fibers or powders. This leads to an increase in the mechanical properties, with Young's modulus reaching (212.1) MPa and compressive strength at (24.3) MPa. On the other hand, the results show that these biocomposites also have acceptable thermal insulation performance, achieving a thermal conductivity of (0.102) W/(m·K), making them suitable for a variety of applications in sustainable buildings and for refurbishment.

Keywords: insulating panels; chamaerops humilis fibers; biodegradable binders; natural materials; physico-mechanical properties

Academic Editor: Hom Nath Dhakal

Received: 14 December 2024
Revised: 28 January 2025
Accepted: 29 January 2025
Published: 2 February 2025

Citation: Elmoudnia, H.; Millogo, Y.; Faria, P.; Jalal, R.; Waqif, M.; Saâdi, L. Development of Doum Palm Fiber-Based Building Insulation Composites with Citric Acid/Glycerol Eco-Friendly Binder. *J. Compos. Sci.* **2025**, *9*, 67. https://doi.org/10.3390/jcs9020067

1. Introduction

The use of Doum palm fiber (DPf) in scientific research has attracted attention due to its unique properties and potential applications in various fields, including in composites [1–3]. DPf, derived from the leaves of the Doum palm tree (Chamaerops humilis), is abundant in the Arabian Peninsula and northern Africa. It is characterized by its low density and favorable mechanical properties, making it a suitable candidate for the reinforcement of polymer matrixes [2,3].

Research has shown that DPf can significantly improve the mechanical, thermal and rheological properties of composites when treated by chemical methods such as alkaline treatment [4–7]. This treatment not only improves the surface characteristics of the fiber, but also increases its cellulose content, which is crucial for better adhesion within the

polymer matrix [8,9]. Studies have shown that incorporating DPfs into polypropylene and gypsum composites results in improved tensile strength and energy absorption capabilities, indicating their effectiveness as a reinforcing material [1]. In recent years, DPfs have been the subject of a great deal of research and have proved to have interesting mechanical and physical properties. These cellulosic fibers have been used to develop applications in the construction and other industries in terms of reinforcement. Fardioui et al. [10] evaluated the potential of this plant to be used as a reinforcement for water-soluble polymers to prepare bio-nanocomposites by studying the effect of chemical treatment on these fibers. A study carried out by Bahloul et al. [11] on DPfs showed that the cellulose nanocrystals produced from these fibers could be used as additives or reinforcing agents in the preparation of polymer composites. Arrakhiz et al. [12] evaluated the thermal and mechanical properties of DPfs reinforcing a low-density polyethylene composite to optimize it. They also studied the effect of an alkaline treatment to clean the fiber surface and improve polymer/fiber adhesion. Essabir et al. [13] have shown that DPfs are an environmentally friendly reinforcement in polymer composites because of their mechanical properties and abundance. Dan-Asabe et al. [14] produced a composite by compression molding, using DPfs as a reinforcement. The authors found that the formulation with the best mechanical properties consisted of 8% DPf, 62% Polyvinyl chloride (PVC) and 30% Kankara clay, resulting in a water absorption rate of 0.72%, a Young's modulus of 2 GPa, a flexural strength of 84 MPa and a density of 1.43 g/cm^3. The possibility of using gypsum mortar reinforced with DPfs as thermal insulation in buildings was evaluated by Fatma [2]. Several composite materials were prepared, and the DPfs were treated with a 1% NaOH solution to improve their resistance to chemical degradation. Improved mechanical performance and thermal conductivity were observed in composites reinforced with treated DPfs, indicating their potential as natural thermal insulators. Bouchefra et al. [15] studied the physical and mechanical properties of compressed earth bricks (CEBs) reinforced with raw DPfs and treated DPfs. The addition of raw and treated DPfs was found to reduce compressive strength by 25% and 35%, respectively, while improving thermal insulation and reducing density by around 16%. The results suggest that the use of DPfs in green composites offers promising prospects for future applications in building.

The growing demand for sustainable materials in various industries has led to significant interest in biobased binders [16,17]. Among these, glycerol/citric acid blends have emerged as promising candidates due to their renewable nature and effective binding properties [18–20]. Both glycerol and citric acid are derived from natural sources, making them environmentally friendly alternatives to traditional synthetic binders. The combination of these two compounds leads to the formation of ester bonds through polymerization reactions, which enhances the adhesive properties of the mixture [16]. Research indicates that the presence of hydroxyl and carboxyl groups in glycerol and citric acid facilitates the creation of three-dimensional polymer structures when subjected to heat and pressure, thereby improving the bonding performance of composites with this binder [21,22]. An important application of citric acid/glycerol acid blends is in the manufacture of jute particleboard [23]. Nitu et al. [23] showed that varying the concentration in the citric acid/glycerol ratio significantly affected the mechanical properties and dimensional stability of the resulting particleboard. Specifically, a blend containing a 20 wt% citric acid/glycerol ratio of 40/60 showed optimum performance, achieving a modulus of rupture of 19.67 N/mm^2 and a thickness swell of 9%, which is in line with industry standards. Fourier transform infrared (FTIR) analysis confirmed the formation of ester bonds, which contributed to improved properties through cross-linking with jute particles. In addition to particleboard, citric acid/glycerol blends have been studied as binders for plywood production [24]. The results indicate that the mechanical properties and water resistance of

plywood are significantly influenced by the pressing temperature rather than the amount of adhesive. Choowang et al. [24] found that, at temperatures of 180 °C to 200 °C, the binder effectively penetrates the wood surface, improving adhesion and overall performance.

To the authors' knowledge, the present study is the first attempt at using DPf as an eco-friendly substitute in the production of insulation boards bonded with a biobased adhesive consisting of citric acid (CA) and glycerol (GLY). While most studies have focused on hot pressing methods, this research aims to provide an understanding of the effects of cold pressing, which can significantly decrease energy consumption and production costs. Through the application of a wide range of analytical techniques (FTIR, XRD, TGA, SEM and EDX), this study contributes to the characterization of the physicochemical properties of DPf and assesses its ability to improve polymer composite performance. The aim is that these findings can impact manufacturing processes in the construction industry, encouraging the implementation of sustainable composites that utilize agricultural by-products to meet the pressing global need for sustainable construction materials and products.

2. Materials and Methods

2.1. Doum Palm Fibers and Binding Materials

The leaves containing the DPfs were collected in the Safi region of Marrakech, Morocco.

Citric acid monohydrate (CA) and purified glycerol (GLY) were the main raw materials chosen to bind the fibers together, with p-toluene sulphonic acid (p-TSA) as the catalyst [25]. The materials and catalyst used for the esterification reaction are identified in Table 1.

Table 1. Identification of binder reagents.

Product	Origin	Molecular Weight (g/mol)	Density (g/cm^3)
Citric acid monohydrate	Sigma-Aldrich	210.14	1.5
Pure glycerol	Lobachemie	92.09	1.26
p-TSA	Sigma-Aldrich	172.20	1.24

Tap water was used.

2.2. Physical Properties of the Fibers

2.2.1. Density and Diameter Measurement

The average diameter of DPfs was assessed using a digital microscope (model: JEOL/JSM-5500). The fibers were placed on a glass slide and taped at the ends to ensure stability during measurement. Diameter measurements were taken at several points, including the middle and both ends of each fiber. In accordance with ASTM D578-79 [26], the density of natural fibers was determined experimentally using a pycnometer filled with a liquid of known density (toluene, 0.866 g/cm^3). Before the test, the untreated fibers were cut to a length of 5 mm after being dried in desiccators filled with silica gel for four days. This preparation provided accurate measurements and reliable data for subsequent analysis.

The density of untreated fibers was calculated using Equation (1).

$$\rho_{DPf} = \left(\frac{m_2 - m_1}{(m_3 - m_1) - (m_4 - m_2)}\right)\rho_{toluene} \quad (1)$$

where

ρ_{DPf} represents the density of the fiber in g/cm^3;

$\rho_{toluene}$ is the density of toluene in g/cm^3;

m_1 is the mass of the empty pycnometer in grams;
m_2 is the mass of the fiber pycnometer in grams;
m_3 is the mass of the toluene-filled pycnometer in grams;
m_4 is the mass of the pycnometer containing the fibers and toluene in grams.

2.2.2. Determination of Chemical Constituents

To analyze the chemical composition of DPf, approximately 40 g of ground fibers was used. Cellulose content was determined using the Kurschner and Hoffer method [4], which specifically measures the percentage of cellulose in the sample. The hemicellulose content was assessed using the Boopathi method [27]. Insoluble lignin content was quantified using the Klason technique [28]. Each of these analytical procedures was repeated three times to ensure the reliability and consistency of the results obtained. This comprehensive analysis provides crucial information on the potential applications of the fibers in various industries, particularly in the development of composites.

2.3. Analysis of X-Ray Diffractograms of the Fibers

X-ray diffraction (XRD) analysis was carried out on DPfs to study their crystallographic properties. The powdered fibers, with a particle size of approximately 200 µm, were analyzed using a Philips X'Pert MPD diffractometer. Measurements were taken at various 2θ angles, with a scan speed of 8°/min and a step size of 0.02°. The XRD installation was operated at a voltage of 40 kV and a current of 40 mA. The aim of this analysis was to provide information on the crystalline structure, crystallinity index and crystallite size of DPfs, which are crucial to understanding their potential applications in composite materials. The diffractogram obtained identified the degree of crystallinity and the arrangement of molecular chains in the fibers, thus contributing to the overall characterization of the material. The Segal method [29] (Equation (2)) was used to calculate the crystallinity index of the DPfs:

$$CrI(\%) = \left(1 - \frac{I_{am}}{I_{002}}\right) \times 100 \quad (2)$$

where I_{002} represents both amorphous and crystalline material, while I_{am} represents only the amorphous part.

The crystallite size (Cs) of the DPfs was estimated using Scherrer's formula [30]:

$$Cs = \frac{k \cdot \lambda}{\beta \cdot \cos\theta} \quad (3)$$

where β is the total width of the peak at half-maximum (200), λ is the wavelength of the X-ray beam, k = 0.89 is the Scherrer constant and θ represents the Bragg angle.

2.4. Morphological Analysis of the Fibers

The microstructure of DPfs was analyzed using a scanning electron microscope (SEM) (model: JEOL/JSM-5500). The examination was carried out at an accelerated voltage of 30 kV, allowing detailed observation of the fiber surfaces at different magnifications. To mitigate the effects of the electron beam charge during imaging, a thin layer of platinum was applied to the DPf samples. In addition, SEM-integrated energy dispersive X-ray spectroscopy (EDX) was used to identify the primary elements present on the fiber surface. Understanding the chemical composition of DPfs is crucial to optimizing their application in composite manufacturing.

2.5. Thermal Stability of the Fibers

The thermal stability of DPfs was assessed using a thermogravimetric analysis and differential thermal analysis (TGA/DTA) system (Setsys 24 Discovery, Setaram Instrumentation, Caluire-et-Cuire, France). Approximately 10 mg of finely ground fibers was placed in an alumina crucible and subjected to a nitrogen atmosphere at a flow rate of 20 mL/min. The temperature was gradually increased from room temperature to 900 °C at a rate of 10 °C/min. This method enabled the thermal degradation characteristics of the DPfs to be assessed and provided valuable information about their stability at elevated temperatures.

2.6. Preparation of the Composites and Specimens

2.6.1. Binder Composition and Preparation

Based on the work of Franz Segovia et al. [25], a ratio of 1:1 (mol/mol) between GLY and CA was used.

Before the specimens were produced, several tests were conducted on the preparation of the binder in order to optimize the kinetic parameters (time and temperature) that influence the reaction.

Glycerol was initially heated to 120 °C before citric acid was added. The solution was stirred vigorously for 120 min until the citric acid was completely dissolved. The mixture was then cooled to 100 °C, and 2% of the catalyst (p-TSA) (by total weight of the mixture) was added. Finally, the solution was cooled to room temperature. Before being used with fibers, the solution was mixed with water at 70 °C to facilitate its application as a binder (Figure 1). The amount of water added can vary depending on the desired viscosity and ease of use.

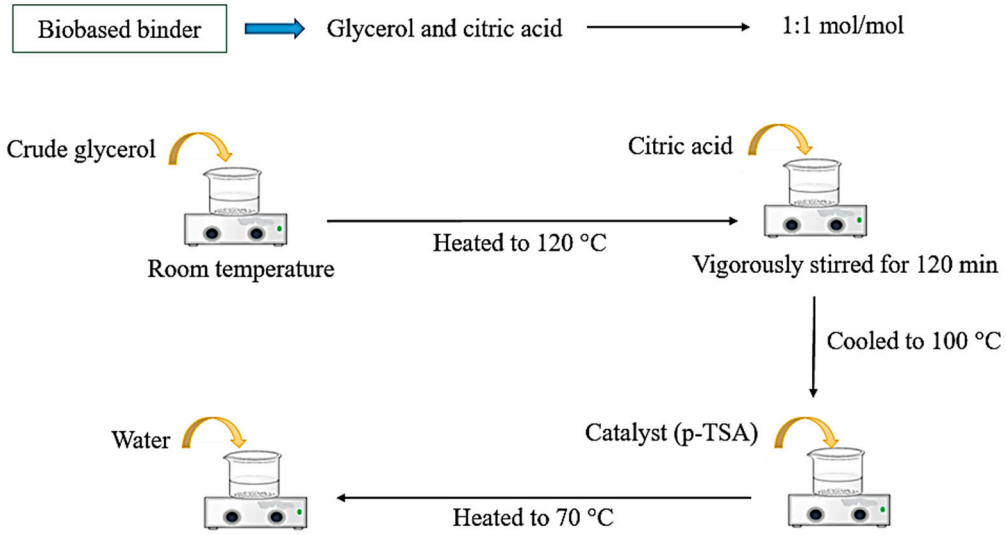

Figure 1. Binder preparation protocol with glycerol, citric acid, water and catalyst, with thermal treatments.

2.6.2. Fiber Preparation

Once the DPfs have been harvested, a preliminary treatment is required to increase their effectiveness. Harvested Doum leaves contain dust and other types of impurities. The fibers were first carefully cleaned to remove all these impurities and foreign bodies so that only clean, usable leaves remained. They were then dried at a temperature of 30 °C for 3 days to ensure a constant moisture content. The fibers were then extracted manually by rubbing the leaves against a rough surface, ensuring complete separation of the fibrous material.

In this study, two sizes of DPfs were prepared to produce test specimens: short fibers (10–17 mm long), and powdered fibers (less than 5 mm long), cut using a Lamacom-type knife mill (Figure 2).

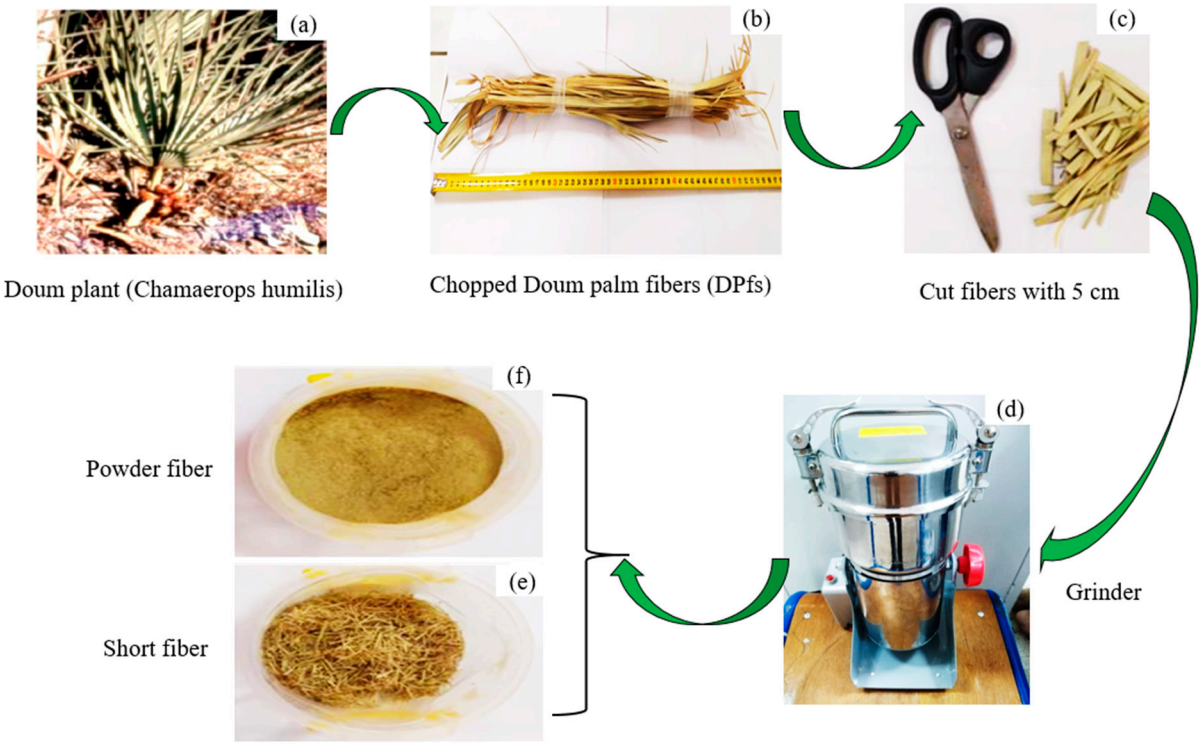

Figure 2. Preparation of the fibers: (**a**) Chamaerops humilis; (**b**) chopped fibers; (**c**) cut fibers; (**d**) mill used to prepare the fibers; (**e**) short and (**f**) powdered fibers.

2.6.3. Composite and Specimen Preparation

First, the binder was applied to the two sizes of DPfs (short fibers and powdered fibers). Subsequently, water was sprayed onto the surface in an amount corresponding to 10% of the particle weight. For the powdered fibers, the binder was added gradually in a controlled ratio. The mixing was carried out manually at room temperature to ensure that the binder evenly coated all the fiber particles. This step is crucial for achieving uniform impregnation, as powdered fibers have a much finer texture compared to short fibers (Figure 3). They were then placed in a cylindrical mold (30 mm diameter, 80 mm high) and immediately compressed using a hydraulic press at 60 bar for 2 min. Finally, the samples were stored at 40 °C until a constant weight was obtained.

Table 2 shows the percentage of binder used, in relation to the mass of fibers (short fibers, DPs, or powder, DPp), for each composite. The B-number defines the % of binder used on the formulation.

Table 2. Biocomposite abbreviations and formulations.

Biocomposite	Binder %	Type of Fiber
DP*s*-B-20	20	Short
DP*s*-B-30	30	
DP*s*-B-40	40	
DP*p*-B-20	20	Powder
DP*p*-B-30	30	
DP*p*-B-40	40	

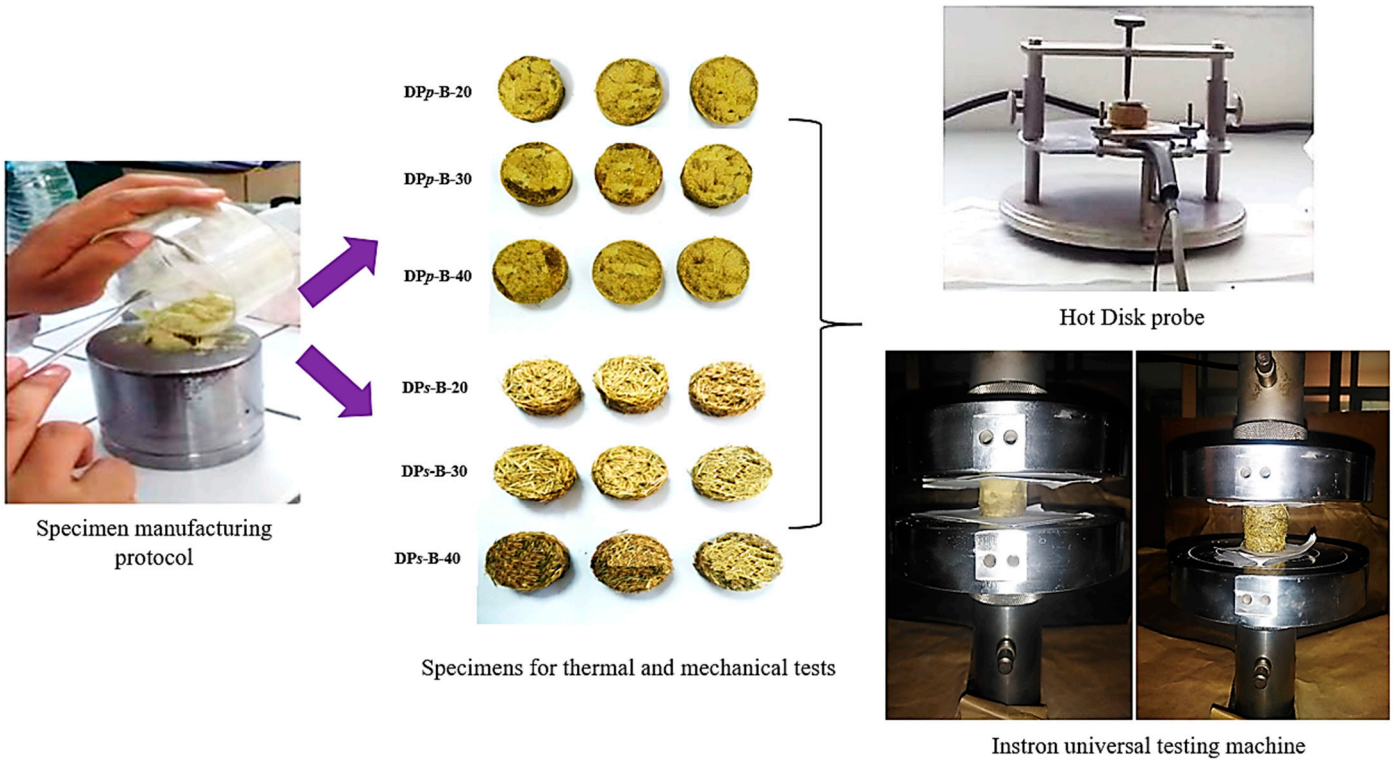

Figure 3. Composite specimens and thermal and mechanical experimental tests carried out.

2.7. Fourier Transform Infrared Analysis of the Fibers and Binder

Fourier transform infrared spectroscopy (FTIR) was used to analyze the functional groups and chemical components present in the DPfs. The fibers were first ground to a fine powder and then mixed with potassium bromide (KBr) powder in a 1:10 ratio (DPf:KBr). This mixture was then pressed into a fine pellet using a hydraulic press, applying a force of 5 tons for 20 s. The prepared sample was placed in the FTIR spectrometer (Vertex 70) for analysis. For liquid binder analysis, a small volume was placed directly on the ATR crystal for spectral analysis.

The FTIR analysis was carried out at room temperature, with 45 spectral scans recorded to obtain the spectrum in the wavelength range from 4000 to 400 cm^{-1} with a resolution of 4 cm^{-1}.

2.8. Thermal Conductivity and Density of the Composites

Thermal characterization of the composites was carried out on HOT-10-TPS 1500 equipment at a temperature of 25 °C (Figure 3).

The density of the biocomposite is defined as the ratio of the sample mass to its volume and is calculated using the following equation:

$$\rho = \frac{m}{V} \tag{4}$$

where m is the sample mass and V is the sample volume. The values measured represent an average of three samples.

2.9. Mechanical Testing of the Composites

The mechanical characterization of the composites produced involved the assessment of compressive strength and Young's modulus. These tests were carried out in accordance with ASTM D 3379-75 [31], using an Instron model 3369 universal testing machine to ensure accurate and reliable results. The equipment features a compression cell consisting of two

parallel hardened stainless steel plates, ensuring uniform application of load during testing. A total of three specimens were tested per formulation.

3. Results

3.1. Physicochemical Analysis of Doum Palm Fibers

The chemical composition and morphological microstructure of plant fibers are extremely complex due to their hierarchical organization and the presence of different compounds in varying concentrations. Table 3 shows the chemical composition obtained by tests performed on the DPfs. The organic matter of DPfs is mainly composed of 38% cellulose, 23.5% hemicellulose, 18.34% lignin and 13 to 15% extractable. The results of this study corroborate those reported in the literature for DPfs, which are as follows: 30–43% cellulose, 18–31% hemicellulose, 23–28% lignin and 12.5% extractable [10,11]. Compared with other fibers, DPfs have a higher organic matter content than Diss and Kenaf fibers, with values of 88.6% and 91.7%, respectively. However, this is lower than those of Alfa (98.6%) and Flax (97.96%) fibers. This difference is probably due to the environment in which the plant is grown, the type of fiber, the age of the plant, the conditions and the period of storage and/or preservation after harvesting [4,32].

Table 3. Chemical compositions and comparison of DPfs with other natural fibers from the literature.

Fiber	Cellulose (%)	Hemicellulose (%)	Lignin (%)	Ash (%)	Density (g/cm^3)	Diameter (µm)	Ref.
DPf	38	23.5	18.34	3.7	1.24	110–270	Current study
Doum leaves	43.2	30.1	23.7	-	-	-	[3]
Doum palm petiole	42.3	21.85	18	-	1.32	353.37 ± 31.49	[2,33]
Doum leaves	30.86	18.57	33.12	2.23	-	3–10	[11]
Doum trunk	29.01	19.74	28.64	4.79	-	3–10	[11]
Doum palm	43.1	35.8	18	-	-	-	[1]
Washingtonia robusta	40	19.34	23.5	5	1.2	260–314	[34]
Oil palm	49.6	18	21.2	-	0.7–1.55	-	[35]
Sugar palm	43.95	8.24	43.81	5.61	-	314.33 ± 55.75	[36]
Phoenix sp.	61.13	12.56	19.91	7.69	1.257	576.6	[37]

Table 4 shows the chemical compositions of DPfs in their raw state. The results show that the water content in the fibers was approximately 6.88%, while the dry matter content was 93.12%, the mineral content was 4.66% and the organic matter content was approximately 95.34%. These results were confirmed by energy dispersive X-ray (EDAX) analysis of the raw fiber, which contains low proportions of mineral matter (Mg, Al, S, Cl, K), as shown in Figure 4.

Table 4. Chemical compositions of DPfs in their raw state.

Components	Organic Matter	Mineral Matter	Dry Matter	Water	Extractable (Ethanol/Toluene)	Extractable (Hot Water)
% by weight	95.34	4.66	93.12	6.88	13	15

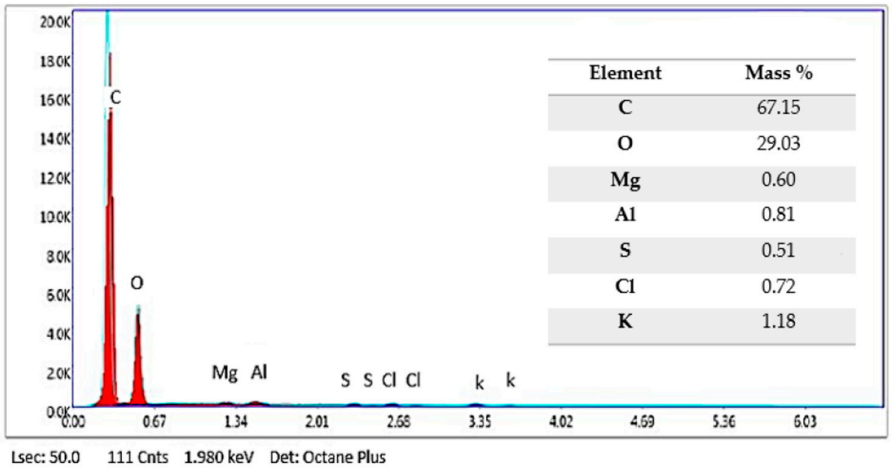

Figure 4. SEM EDX analysis of DPfs.

3.2. Fourier Transform Infrared (FTIR) Analysis

Figure 5 shows the infrared bands of DPfs in their raw state. The bands obtained have been attributed to the main components of natural fibers, such as cellulose, hemicellulose and lignin. The broad band observed in the 3600–3100 cm^{-1} region indicates vibration of the O-H bond. This broad and extended band is typical of plant fibers (lignocellulosic) due to the extensive inter-/intra-molecular OH bond attached to the structures of cellulose, hemicellulose and lignin [38–41]. The bands observed at 2923 and 2864 cm^{-1} are attributed to the vibration of the C-H bonds of the CH and CH_2 groups, respectively, which are present in cellulose, hemicellulose and lignin [13,42–44]. The band observed at 1738 cm^{-1} indicates the elongation vibration of the C=O carbonyl group, which is present in hemicellulose and/or lignin as well as in pectin [4,45,46]. The band at 1648 cm^{-1} is mainly associated with the binding vibration of water molecules absorbed in the cellulose structure [4,45]. The band at 1515 cm^{-1} is attributed to the C=C vibrations of the aromatic ring present in hemicellulose and lignin. The bands at 1460 and 1382 cm^{-1} correspond, respectively, to the CH_2 elongation vibration and the OH deformation of cellulose [47–49]. The band at 1243 cm^{-1} corresponds to the C-O vibration of the acetyl group in hemicellulose [50–52]. The C-O-C and C-O-H vibrations of cellulose are located at 1150 and 1050 cm^{-1}, respectively [52–54]. Finally, the band at 897 cm^{-1} is due to C-O-C, attributed to the β-(1→4) glycosidic bonds present in cellulose [11,54,55].

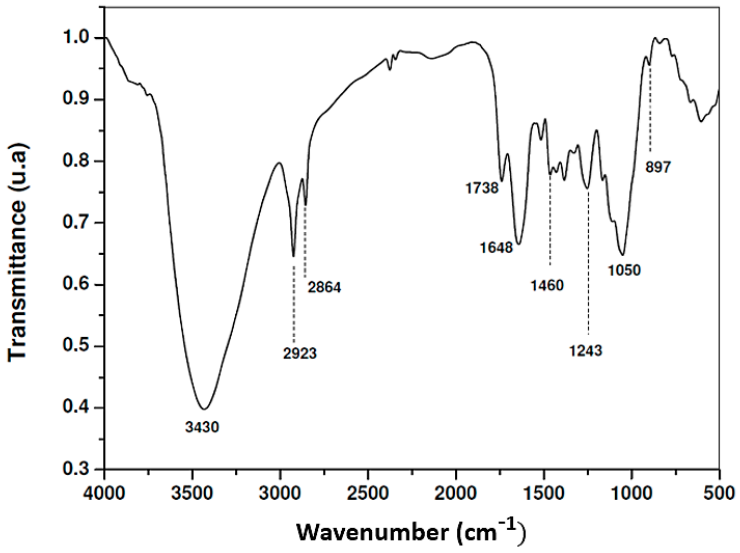

Figure 5. FTIR spectra of DPfs in the raw state.

3.3. X-Ray Diffraction (XRD) Analysis

The diffractogram (Figure 6) of the raw DPfs showed lines characteristic of the typical structure of cellulose I. The latter is characterized by the main crystalline peaks located at approximately 14.9°, 16.3°, 21.4° and 34.4°, corresponding to the (1–10), (110), (200) and (004) typical reflection planes [34]. Several researchers have found that the position of the peak corresponding to the (200) crystallographic plane is approximately 2θ = 22.3°. However, in the case of the DPfs studied, this same peak was shifted to lower angles. This may indicate the presence of another polymorph, possibly cellulose IV. Thus, it appears that the lateral disorganization of cellulose I led to the cellulose IV polymorph [44,56].

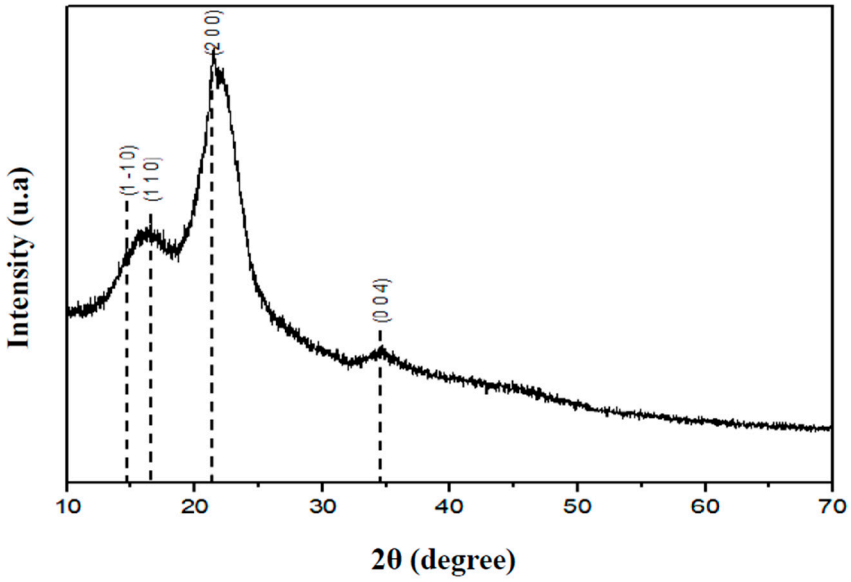

Figure 6. X-ray diffractogram of DPfs in the raw state.

The estimated crystallinity index (CI) for DPf is 54%, which is higher than that for *Pennisetum alopecuroides* (49.14%), *Phoenix pusilla* (42.6%), sugar palm (42.28%), *Elettaria cardamomum* (36.84%) and *Washingtonia robusta* palm (40%) [4,34,36,57,58]. However, the crystallite size (CS) of DPf was calculated to be 5.2 nm using Equation (3).

3.4. Thermal Analysis (ATG-ATD)

Several studies have examined the effect of temperature on cellulose, hemicellulose and lignin in different types of fibers [51,59–62]. They indicated that hemicellulose decomposes at a maximum of 290 °C, while lignin decomposes thermally with peaks of 280 to 520 °C. Thermal cellulose decomposition begins at 210–260 °C by dehydration, followed by a major endothermic depolymerization reaction with peaks ranging from 310 to approximately 450 °C [63–65].

The thermal behavior of the DPfs was studied by thermogravimetric analysis (TGA) (Figure 7). Three weight losses are observed resulting from the decomposition of the different components of the fiber studied. The first weight loss is about 4.79% at 84 °C, attributed to the release of moisture-related water absorbed on the surface of a hydrophilic lignocellulosic structure [34,61]. The second significant weight loss is about 23.91% at 260 °C, related to the decomposition of hemicellulose and pectin and cleavage of cellulose glycosidic bonds [8,55,65]. The third weight loss (50% by weight) is noted at 305 °C and could be attributed to the breakdown of cellulose and lignin [59,66]. These results are in line with several studies that have referred to the thermal stability of natural fibers [34,67–72].

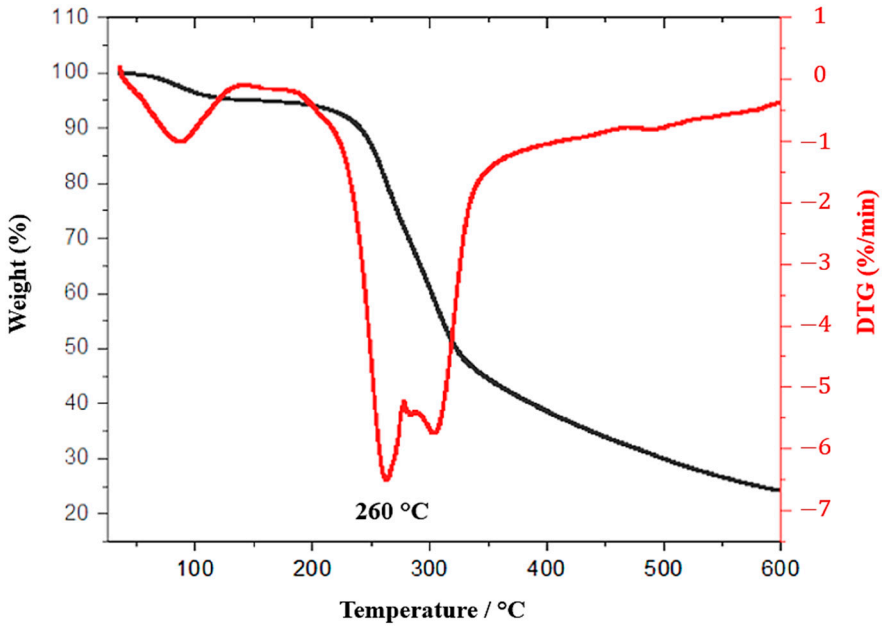

Figure 7. ATG-ATD curves of raw DPfs.

3.5. Morphological Analysis by SEM

The surface morphology of DPfs, as shown in the SEM images (Figure 8), has characteristics typical of natural fibers. These fibers have a network of fibrils interconnected over their entire length by pectin and various non-cellulosic substances. This unique structure contributes to the overall mechanical properties of the fibers, thus enhancing their potential for use in composite materials [11,73,74]. The presence of these bonding compounds plays a crucial role in maintaining fiber integrity and functionality, as has been observed for other types of natural fibers [75–78].

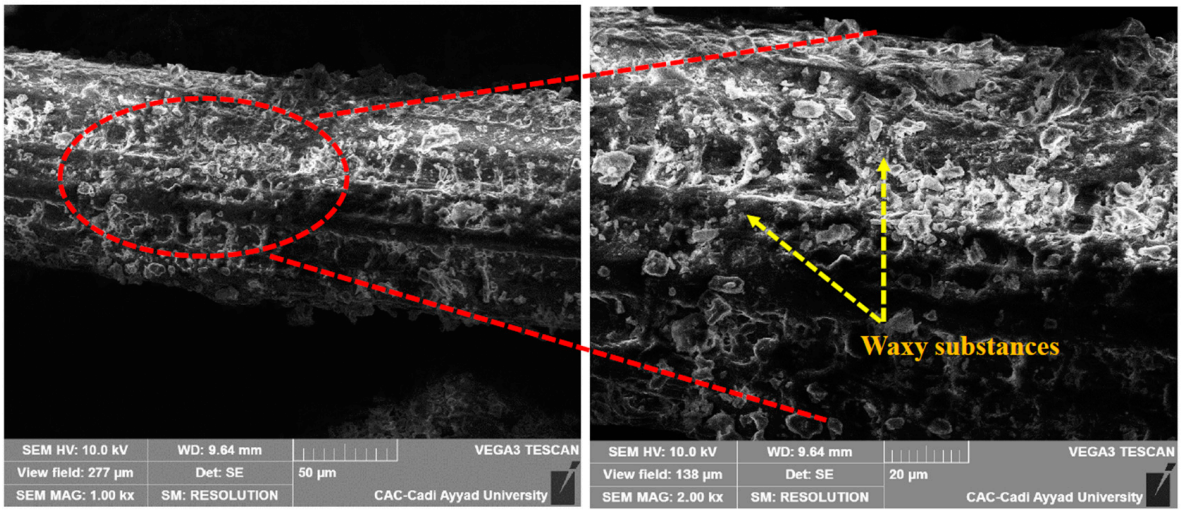

Figure 8. SEM observation of untreated DPfs.

3.6. Characterization of the Binder and Biocomposites

The binder was characterized by Fourier transform infrared analysis (FTIR) to confirm the presence of esters. Several mechanical and thermal tests were also performed to select the appropriate formulation.

The structure of the ester was confirmed by FTIR peaks, whose characteristic bands are shown in Figure 9. A wide band at 3427 cm^{-1} is characteristic for hydroxyl groups of alcohols and acids, indicating incomplete conversion of hydroxyl groups in reagents [71,79].

The 2957 cm^{-1} band is characteristic of polyester C-H vibrations. The narrow band at 1738 cm^{-1} is characteristic of the carbonyl group, the narrow band at 1190 cm^{-1} is characteristic of the acyl group and the low band at 1045 cm^{-1} is characteristic of the alcoxy group. These bands prove that a polyester was obtained [25,80–82].

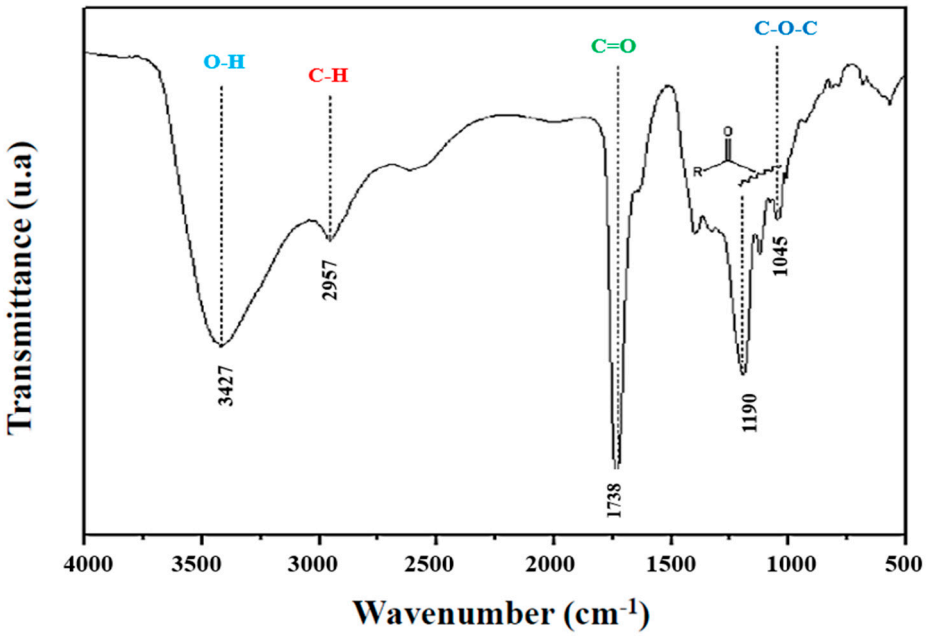

Figure 9. Infrared spectrum of the biosourced binder synthesized based on CA-GLY.

The irreversibility of condensates is assumed to be due to high reaction temperatures, which allow for rapid evaporation of water, thus shifting the equilibrium point towards the products [80] (Figure 10). When the temperature exceeds 100 °C, water is discharged as vapor, which promotes polymerization. While polymerization begins at temperatures above 100 °C, it occurs more rapidly at higher temperatures. At moderate temperatures slightly above 100 °C, the curing process can last several hours (for instance, one night), while at temperatures between 175 and 200 °C, the curing process can be completed in 30 min to 1 h [19].

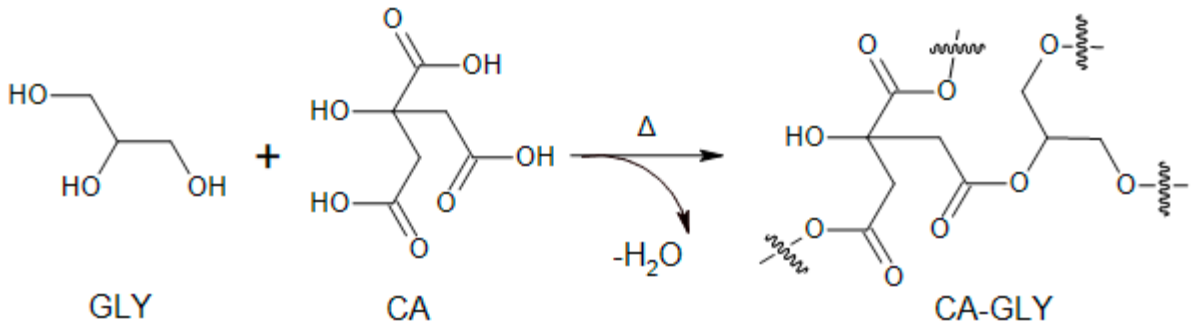

Figure 10. Reactions involving both citric acid and glycerol molecules in condensation.

3.7. Mechanical and Physical Characterizations of Biocomposites

3.7.1. Mechanical Properties

The biocomposites' compressive strength and Young's modulus are shown in Table 5.

Table 5. Biocomposites' compressive strength and Young's modulus.

Biocomposite	Compressive Strength (MPa)	Young's Modulus (MPa)	Dimensions (Ø × e) (mm^2)
DP*s*-B-20	24.32 ± 2.54	210.63 ± 10.66	30 × 36
DP*s*-B-30	21.20 ± 0.98	212.14 ± 6.35	30 × 35
DP*s*-B-40	10.74 ± 1.94	117.78 ± 3.85	30 × 34
DP*s* range	18.75 ± 1.82	180.14 ± 6.95	-
DP*p*-B-20	12.04 ± 1.74	79.52 ± 5.66	30 × 25
DP*p*-B-30	7.61 ± 0.31	43.42 ± 3.52	30 × 22
DP*p*-B-40	5.74 ± 0.51	26.50 ± 3.53	30 × 20
DP*p* range	8.35 ± 0.85	49.81 ± 4.23	-

Figure 11a,b show the evolution of the compressive strength and the Young's modulus in compression of specimens of the different formulations studied. It is observed that the mechanical properties are affected by the variation in the proportion of the binder and by the size of the DPfs. The results indicate that the increase in binder quantity decreased the compressive strength and the Young's modulus of the specimens in both cases (short fibers and powdered fibers). It appears that the short-fiber (DPs) specimens have higher values than those based on powdered fibers (DPp) in all cases, particularly with the proportions of 20% and 30% of binder. The measured compressive strength for the DPs biocomposite ranged from 24.32 MPa to 10.74 MPa depending on the amount of binder. In contrast, the samples made of DPp achieved lower compressive strength values, always below 12 MPa. Previously, researchers found that reinforcing composites with longer natural fibers such as sugarcane, coconut and cotton to improve the properties of the composite boards was preferred because they could create a better fiber network through particle overlap, enhancing the mechanical properties of the composite boards [83–85].

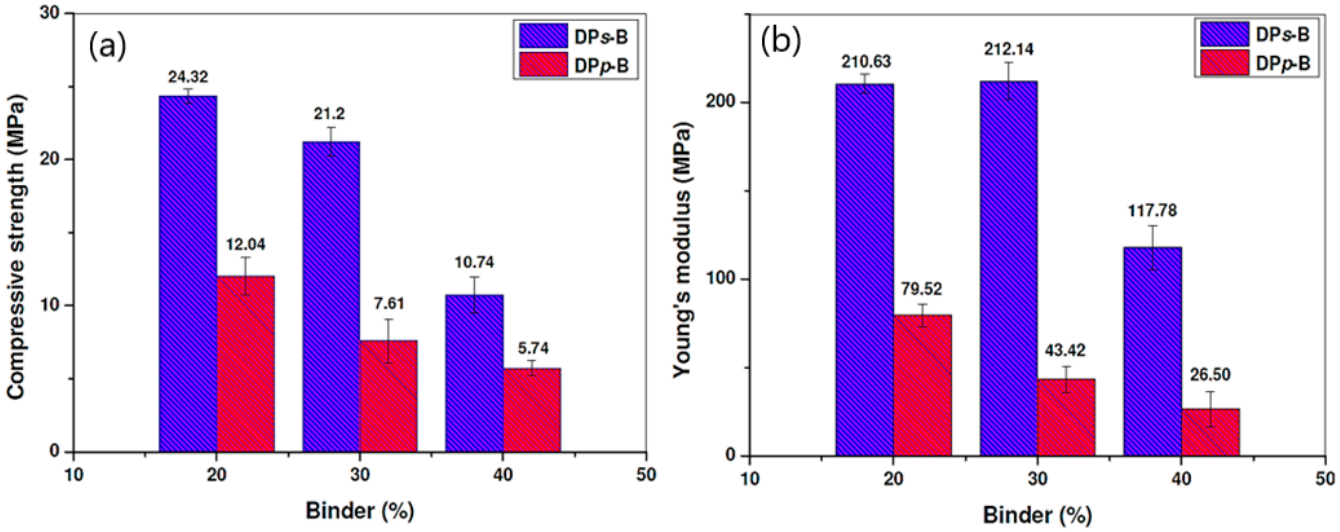

Figure 11. Mechanical properties of DPf-based specimens at different sizes with b-average and standard deviation: (**a**): compressive strength; (**b**): Young's modulus.

The higher Young's modulus was achieved by only using DPss with a low binder ratio, which is attributed to the size of the fibers and the binder ratio. When the fibers are long, they give the sample flexibility due to interlacing of the fibers with each other, which delays its rupture [86]. These results are consistent with those of several researchers [86–88]. Indeed, increasing the amount of binder can create a less cohesive structure, resulting in a weaker interfacial bond between the fibers and binder. When there is too much binder, it can fill the gaps between the fibers instead of contributing to reinforcement,

resulting in a decrease in compressive strength and Young's modulus. These findings were compatible with the study conducted by Tigabe et al. [89]. Fiber size also plays a crucial role in determining mechanical performance [90]. Short fibers tend to provide better reinforcement than powdered ones because they can transfer loads efficiently through the fiber/matrix interface. The larger contact area and better alignment of short fibers allow for more efficient stress distribution in the composite. A larger contact area between fibers in a composite allows for better interaction and bonding between the fibers and the matrix, resulting in higher values for compressive strength and Young's modulus [91].

The binder viscosity is another key element, as it relates to how it flows over the surfaces of the fibers. Some studies [92–94] indicate that binder viscosity significantly influences the mechanical performance of composites. Binders with optimal viscosity enhance the modulus of rupture and modulus of elasticity in particleboards by ensuring effective bonding between fibers and the matrix. Conversely, excessively high or low viscosity can affect adhesion, leading to reduced mechanical strength. This highlights the importance of selecting appropriate binder viscosity to optimize natural fiber-reinforced composite performance.

3.7.2. Physical Properties

The thermal conductivity and density are given in Table 6.

Table 6. Values of thermal conductivity and density, ranges by type of DPf used and comparison to other insulation materials.

Composites	Density (g/cm^3)	Thermal Conductivity W·m^{-1}·K^{-1}	Dimension (Ø × e)	Source
DP*s*-B-20	0.507	0.1283	30 × 18 mm^2	Current study
DP*s*-B-30	0.506	0.1158	30 × 11 mm^2	Current study
DP*s*-B-40	0.450	0.1022	30 × 10 mm^2	Current study
DP*s*-B-20 to 40	0.488	0.1154	-	Current study
DP*p*-B-20	0.868	0.2173	30 × 16 mm^2	Current study
DP*p*-B-30	0.916	0.2062	30 × 10 mm^2	Current study
DP*p*-B-40	0.877	0.2137	30 × 10 mm^2	Current study
DP*p*-B-20 to 40	0.887	0.2124	-	Current study
Corn cob particleboard	0.171–0.334	0.101	25 × 25 × 3 cm^3	[95]
Mineral wool (fiberglass and rockwool)	0.024–0.2	0.025–0.047	30 × 30 × 5 cm^3	[96]
Hemp concrete	0.417–0.551	0.179–0.485	50 × 50 × 50 mm^3	[97]
Wood (pine, lauan)	0.45–0.63	0.15	-	[98]
Hardboard	0.89	0.126	-	[98]
Plywood	0.49	0.083	-	[98]
Water hyacinth particleboard	0.251	0.047	150 × 150 × 15 mm^3	[99]
Particleboard	0.69	0.097	-	[98]
A. donax composite	0.517 ± 0.068	0.128	50 × 50 × 4 cm^3	[100]
Hazelnut shell composite	0.677 ± 0.047	-	10 × 4 cm^2	[101]
Hazelnut shell boards	0.702 ± 0.025	0.16 ± 0.01	10 × 4 cm^2	[102]
Vitis vinifera particleboard	0.782	0.064	600 × 400 × 7.5 mm^3	[103]

Thermal Conductivity

The main property of building insulation materials is thermal conductivity. The aim is to achieve the lowest possible thermal conductivity. The thermal conductivity is shown in Table 6 and Figure 12. All biocomposites remained within the acceptable thermal conductivity range, as they were compared to the threshold of $\lambda < 1.15\ W{\cdot}m^{-1}{\cdot}K^{-1}$, which is regarded as the limit for suitable insulation materials [104]. The results show that thermal conductivity decreases with increasing binder proportion in the case of short and powdered DPfs. DPss have better thermal conductivity compared to DPps, with values ranging from 0.10–0.12 $W{\cdot}m^{-1}{\cdot}K^{-1}$, depending on the proportion of binder. This is in line with the results of Tůmová et al. [86], who studied the effect of straw fiber size on the thermal conductivity of biocomposites. Indeed, when the proportion of binder increases, it fills the spaces between the fibers, which can lead to a more dense composite structure. Excess binder can lead to a less cohesive matrix, negatively affecting the composite's thermal conductivity. While some trapped air bubbles enhance insulation due to air's low thermal conductivity, too much binder can fill gaps between fibers, increasing effective heat transfer pathways and decreasing thermal resistance. Air is a poor heat conductor (0.025 $W{\cdot}m^{-1}{\cdot}K^{-1}$), and these trapped air bubbles can improve insulation properties [87,105,106]. Short fibers tend to align better and create a more uniform structure, which allows for more efficient load transfer and reduces heat conduction pathways. On the other hand, powdered fibers can cause increased porosity and voids, which helps in reducing thermal conductivity. Thus, achieving an optimal binder balance is essential for maximizing both mechanical strength and thermal conductivity.

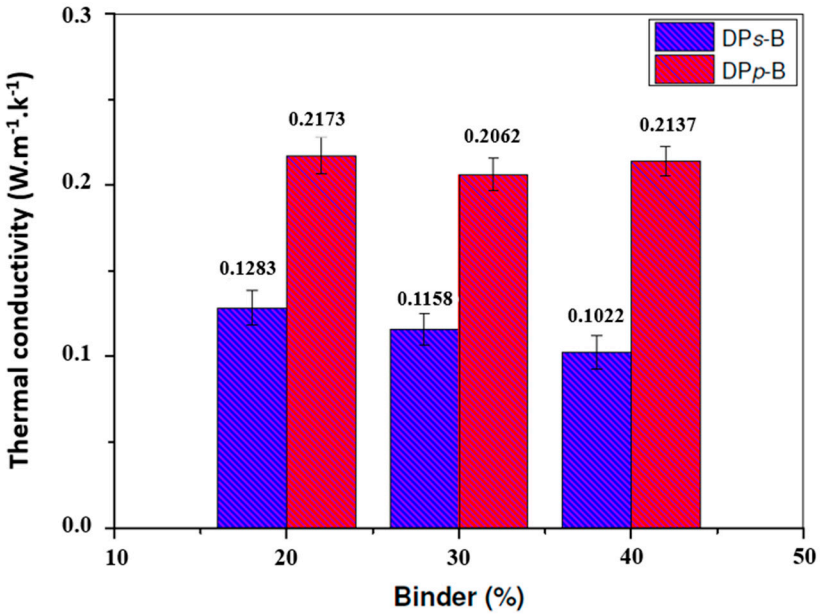

Figure 12. Thermal conductivity of Doum fiber-based test pieces at various sizes.

The thermal conductivity of DPf composites is in the same range as some environmentally friendly insulation composites available on the market, namely hemp concrete (0.17–0.48 $W{\cdot}m^{-1}{\cdot}K^{-1}$), cocoa fiber insulation boards (0.10 $W{\cdot}m^{-1}{\cdot}K^{-1}$) and date palm fiber insulation boards (0.15 $W{\cdot}m^{-1}{\cdot}K^{-1}$) [97,107,108]. However, they are less performant than commercial insulating materials such as those based on wood fibers (0.064–0.066 $W{\cdot}m^{-1}{\cdot}K^{-1}$) [86], sunflower fibers (0.088 $W{\cdot}m^{-1}{\cdot}K^{-1}$) [109], rockwool (0.04 $W{\cdot}m^{-1}{\cdot}K^{-1}$), mineral wool (0.036 $W{\cdot}m^{-1}{\cdot}K^{-1}$) and glass fiber (0.035 $W{\cdot}m^{-1}{\cdot}K^{-1}$) [96].

Density

Table 6 shows the variation in density of the different biocomposites.

The DPps have a larger surface area relative to their volume than DPss. This increased surface area allows the fibers in the composite material to be thickened. Therefore, samples made from DPps have higher density values (ranging from 0.868 to 0.917 g/cm^3) because fine particles can fill voids more efficiently and create a more compact structure [87,110]. However, the increase in porosity decreases the density of the sample, which is crucial to understanding the differences in density. Short fibers tend to create more voids and air bubbles in the composite due to their length and arrangement. These voids contribute to a reduction in the overall density (from 0.450 to 0.507 g/cm^3) by reducing the mass per unit volume of the biocomposite. Similar observations have been made by several other researchers [111,112]. The finer, powdered fibers, on the other hand, minimize these voids and allow a denser composite to be obtained. Although the variation in binder ratio has an effect on density, this impact is described as "mild" [89,113–115]. The binder is used to bind the fibers together and fill in the gaps between them. However, its contribution to the overall density may be less than the inherent properties of the fibers themselves. The binder may add some mass, but if it does not significantly alter the structure or the porosity of the composite, its effect on density is minimal [105,116]. Finally, the nature of the fibers also plays a role in determining the density. Different types of fibers, raw and depending on preparation, have distinct physical properties (for example, density, water content) that can influence how they interact with the binder and with each other during processing. Due to their structural composition, DPss may have lower density than DPps [33,117,118].

4. Conclusions

This study demonstrates the potential of Doum palm fibers (DPfs) as an effective reinforcement for citric acid and glycerol binder-based insulation biocomposites. A moderate addition of binder strengthens the fiber bond, while increased fiber content substantially improves the Young's modulus and compressive strength. An analysis of DPf properties reveals that fiber properties and binder proportions are crucial for the biocomposite's performance.

Specifically, powdered fibers create denser composites (0.868 to 0.917 g/cm^3) compared to short fibers (0.450 to 0.507 g/cm^3), as they reduce voids and air cavities that affect density. While variations in binder proportions also influence density, their impact is minor compared to the intrinsic properties of the fibers. The physical characteristics of the fibers, such as thermal conductivity and density, influence their interaction with the binder during processing. DPs composites exhibit lower density than DPps due to fiber size. The thermal conductivity of insulating biocomposites ranged from 0.1022 W·m^{-1}·K^{-1} to 0.2173 W·m^{-1}·K^{-1}. The results were comparable to those for some sustainable thermal insulation materials, although higher than for synthetic ones.

Overall, these results underscore the importance of selecting appropriate fiber preparation and binder ratios for innovative biocomposite development. Furthermore, they suggest avenues for future research aimed at optimizing waste fiber processing to enhance environmentally friendly products for ecological, affordable, efficient and compatible applications for new buildings and for refurbishing existing ones.

Author Contributions: Conceptualization, H.E.; methodology, H.E.; investigation, H.E.; writing—original draft, H.E.; writing—review and editing, H.E.; validation, P.F., Y.M., R.J.; M.W. and L.S; visualization, P.F., Y.M., R.J., M.W. and L.S; supervision, P.F., Y.M., R.J., M.W. and L.S. All authors have read and agreed to the published version of the manuscript.

Funding: This research was supported by the NOVA School of Science and Technology, CERIS, Department of Civil Engineering, Lisbon, Portugal.

Data Availability Statement: Data will be made available on request.

Acknowledgments: The authors would like to acknowledge their sincere thanks to the support provided by the centre d'analyse et de caractérisation (CAC) of Caddi Ayyad university.

Conflicts of Interest: The authors declare that they have no known competing financial interests or personal relationships that could have appeared to influence the work reported in this paper.

References

1. Bougtaib, K.; Jamil, Y.; Nasla, S.; Gueraoui, K.; Cherraj, M. Compressed Earth Blocks Reinforced with Fibers (Doum Palm) and Stabilized with Lime: Manual Compaction Procedure and Influence of Addition on Mechanical Properties and Durability. *JP J. Heat Mass Transf.* **2022**, *26*, 157–177. [CrossRef]
2. Fatma, N.; Allègue, L.; Salem, M.; Zitoune, R.; Zidi, M. The Effect of Doum Palm Fibers on the Mechanical and Thermal Properties of Gypsum Mortar. *J. Compos. Mater.* **2019**, *53*, 2641–2659. [CrossRef]
3. Fardioui, M.; Guedira, T.; Qaiss, A.E.K.; Bouhfid, R. A Comparative Study of Doum Fiber and Shrimp Chitin Based Reinforced Low Density Polyethylene Biocomposites. *J. Polym. Environ.* **2018**, *26*, 443–451. [CrossRef]
4. Elmoudnia, H.; Faria, P.; Jalal, R.; Waqif, M.; Saâdi, L. Effectiveness of Alkaline and Hydrothermal Treatments on Cellulosic Fibers Extracted from the Moroccan Pennisetum Alopecuroides Plant: Chemical and Morphological Characterization. *Carbohydr. Polym. Technol. Appl.* **2023**, *5*, 100276. [CrossRef]
5. Maguteeswaran, R.; Prathap, P.; Satheeshkumar, S.; Madhu, S. Effect of Alkali Treatment on Novel Natural Fiber Extracted from the Stem of Lankaran Acacia for Polymer Composite Applications. *Biomass Convers. Biorefinery* **2024**, *14*, 8091–8101. [CrossRef]
6. Bijlwan, P.P.; Prasad, L.; Sharma, A.; Gupta, M.K.; Kumar, V. Experimental Study on the Mechanical and Hygroscopic Properties of Alkaline-Treated Grewia Optiva/Basalt Fiber-Reinforced Polymer Composites. *Biomass Convers. Biorefinery* **2023**, *14*, 25961–25971. [CrossRef]
7. Njoku, C.E.; Omotoyinbo, J.A.; Alaneme, K.K.; Daramola, M.O. Characterization of Urena Lobata Fibers after Alkaline Treatment for Use in Polymer Composites. *J. Nat. Fibers* **2022**, *19*, 485–496. [CrossRef]
8. Sanjay, M.; Siengchin, S.; Parameswaranpillai, J.; Jawaid, M.; Pruncu, C.I.; Khan, A. A Comprehensive Review of Techniques for Natural Fibers as Reinforcement in Composites: Preparation, Processing and Characterization. *Carbohydr. Polym.* **2019**, *207*, 108–121.
9. Sanjay, M.R.; Madhu, P.; Jawaid, M.; Senthamaraikannan, P.; Senthil, S.; Pradeep, S. Characterization and Properties of Natural Fiber Polymer Composites: A Comprehensive Review. *J. Clean. Prod.* **2018**, *172*, 566–581. [CrossRef]
10. Fardioui, M.; Stambouli, A.; Gueddira, T.; Dahrouch, A.; Qaiss, A.E.K.; Bouhfid, R. Extraction and Characterization of Nanocrystalline Cellulose from Doum (*Chamaerops humilis*) Leaves: A Potential Reinforcing Biomaterial. *J. Polym. Environ.* **2016**, *24*, 356–362. [CrossRef]
11. Bahloul, A.; Kassab, Z.; Aziz, F.; Hannache, H.; Bouhfid, R.; Qaiss, A.E.K.; Oumam, M.; El Achaby, M. Characteristics of Cellulose Microfibers and Nanocrystals Isolated from Doum Tree (*Chamaerops humilis* Var. Argentea). *Cellulose* **2021**, *28*, 4089–4103. [CrossRef]
12. Arrakhiz, F.; El Achaby, M.; Malha, M.; Bensalah, M.; Fassi-Fehri, O.; Bouhfid, R.; Benmoussa, K.; Qaiss, A. Mechanical and Thermal Properties of Natural Fibers Reinforced Polymer Composites: Doum/Low Density Polyethylene. *Mater. Des.* **2013**, *43*, 200–205. [CrossRef]
13. Essabir, H.; Elkhaoulani, A.; Benmoussa, K.; Bouhfid, R.; Arrakhiz, F.; Qaiss, A. Dynamic Mechanical Thermal Behavior Analysis of Doum Fibers Reinforced Polypropylene Composites. *Mater. Des.* **2013**, *51*, 780–788. [CrossRef]
14. Dan-Asabe, B.; Yaro, S.; Yawas, D. Micro-Structural and Mechanical Characterization of Doum-Palm Leaves Particulate Reinforced PVC Composite as Piping Materials. *Alex. Eng. J.* **2018**, *57*, 2929–2937. [CrossRef]
15. Bouchefra, I.; Bichri, F.Z.E.; Chehouani, H.; Benhamou, B. Mechanical and Thermophysical Properties of Compressed Earth Brick Rienforced by Raw and Treated Doum Fibers. *Constr. Build. Mater.* **2022**, *318*, 126031. [CrossRef]
16. Hussin, M.H.; Abd Latif, N.H.; Hamidon, T.S.; Idris, N.N.; Hashim, R.; Appaturi, J.N.; Brosse, N.; Ziegler-Devin, I.; Chrusiel, L.; Fatriasari, W. Latest Advancements in High-Performance Bio-Based Wood Adhesives: A Critical Review. *J. Mater. Res. Technol.* **2022**, *21*, 3909–3946. [CrossRef]
17. Arias, A.; González-Rodríguez, S.; Barros, M.V.; Salvador, R.; de Francisco, A.C.; Piekarski, C.M.; Moreira, M.T. Recent Developments in Bio-Based Adhesives from Renewable Natural Resources. *J. Clean. Prod.* **2021**, *314*, 127892. [CrossRef]
18. Essoua Essoua, G.G.; Landry, V.; Beauregard, R.; Blanchet, P. Pine Wood Treated with a Citric Acid and Glycerol Mixture: Biomaterial Performance Improved by a Bio-Byproduct. *BioResources* **2016**, *11*, 3049–3072. [CrossRef]
19. Kudahettige-Nilsson, R.L.; Ullsten, H.; Henriksson, G. Plastic Composites Made from Glycerol, Citric Acid, and Forest Components. *BioResources* **2018**, *13*, 6600–6612. [CrossRef]

20. Jiugao, Y.; Ning, W.; Xiaofei, M. The Effects of Citric Acid on the Properties of Thermoplastic Starch Plasticized by Glycerol. *Starch-Stärke* **2005**, *57*, 494–504. [CrossRef]
21. Halpern, J.M.; Urbanski, R.; Weinstock, A.K.; Iwig, D.F.; Mathers, R.T.; Von Recum, H.A. A Biodegradable Thermoset Polymer Made by Esterification of Citric Acid and Glycerol. *J. Biomed. Mater. Res. Part A* **2014**, *102*, 1467–1477. [CrossRef] [PubMed]
22. Giroto, A.S.; Valle, S.F.; Borges, R.; Colnago, L.A.; Ribeiro, T.S.; Jablonowski, N.D.; Ribeiro, C.; Mattoso, L.H. Revealing the Structure Formation on Polyglycerol Citrate Polymers—An Environmentally Friendly Polyester as a Seed-Coating Material. *Polymers* **2023**, *15*, 4303. [CrossRef]
23. Nitu, I.P.; Rahman, S.; Islam, M.N.; Ashaduzzaman, M.; Shams, M.I. Preparation and Properties of Jute Stick Particleboard Using Citric Acid–Glycerol Mixture as a Natural Binder. *J. Wood Sci.* **2022**, *68*, 30. [CrossRef]
24. Choowang, R.; Luengchavanon, M.; Raknarong, J. Employing a Mixture of Fine-Particle PKS, Glycerol, and Citric Acid as an Eco-Friendly Binder for Plywood Production from Rubberwood (*Hevea brasiliensis*) Veneer. *J. Wood Sci.* **2024**, *70*, 31. [CrossRef]
25. Segovia, F.; Blanchet, P.; Auclair, N.; Essoua Essoua, G.G. Thermo-Mechanical Properties of a Wood Fiber Insulation Board Using a Bio-Based Adhesive as a Binder. *Buildings* **2020**, *10*, 152. [CrossRef]
26. *ASTM D578*; Standard Specification for Glass Fiber Strands. ATSM: West Conshohocken, PA, USA, 2011.
27. Boopathi, L.; Sampath, P.S.; Mylsamy, K. Investigation of Physical, Chemical and Mechanical Properties of Raw and Alkali Treated Borassus Fruit Fiber. *Compos. Part B Eng.* **2012**, *43*, 3044–3052. [CrossRef]
28. *ASTM 1106-96*; Standard Test Method for Acid-Insoluble Lignin in Wood. ASTM International: West Conshohocken, PA, USA, 2013.
29. Segal, L.; Creely, J.J.; Martin Jr, A.E.; Conrad, C.M. An Empirical Method for Estimating the Degree of Crystallinity of Native Cellulose Using the X-Ray Diffractometer. *Text. Res. J.* **1959**, *29*, 786–794. [CrossRef]
30. Scherrer, P. Bestimmung Der Grosse Und Inneren Struktur von Kolloidteilchen Mittels Rontgenstrahlen. *Nach Ges Wiss Gott.* **1918**, *2*, 8–100.
31. *ASTM D 3379-75*; Standard Test Method for Tensile Strength and Young's Modulus for High-Modulus Single-Filament Materials. ASTM International: West Conshohocken, PA, USA, 1998.
32. Elmoudnia, H.; Faria, P.; Jalal, R.; Waqif, M.; Saâdi, L. A Comprehensive Review on Washingtonia Plant Biomass Fiber in Insulating Materials. *EDP Sci.* **2025**, *601*, 00069. [CrossRef]
33. Naiiri, F.; Lamis, A.; Mehdi, S.; Redouane, Z.; Mondher, Z. Performance of Lightweight Mortar Reinforced with Doum Palm Fiber. *J. Compos. Mater.* **2021**, *55*, 1591–1607. [CrossRef]
34. Elmoudnia, H.; Faria, P.; Jalal, R.; Waqif, M.; Saâdi, L. A Comprehensive Chemical, Physical, Mechanical, and Thermal Characterization of Novel Cellulosic Plant Extracted from the Petiole of Washingtonia Robusta Fibers. *Biomass Convers. Biorefinery* **2024**, 1–17. [CrossRef]
35. Jawaid, M.; Khalil, H.A.; Hassan, A.; Dungani, R.; Hadiyane, A. Effect of Jute Fibre Loading on Tensile and Dynamic Mechanical Properties of Oil Palm Epoxy Composites. *Compos. Part B Eng.* **2013**, *45*, 619–624. [CrossRef]
36. Leman, Z.; Zainudin, E.S.; Ishak, M.R. Effectiveness of Alkali and Sodium Bicarbonate Treatments on Sugar Palm Fiber: Mechanical, Thermal, and Chemical Investigations. *J. Nat. Fibers* **2018**, *17*, 877–889.
37. Rajeshkumar, G. Characterization of Surface Modified Phoenix Sp. Fibers for Composite Reinforcement. *J. Nat. Fibers* **2021**, *18*, 2033–2044. [CrossRef]
38. Adeosun, S.; Akpan, E.; Akanegbu, H. Thermo-Mechanical Properties of Unsaturated Polyester Reinforced with Coconut and Snail Shells. *Int. J. Compos. Mater.* **2015**, *5*, 52–64.
39. Hossain, S.; Jalil, M.A.; Islam, T.; Rahman, M.M. A Low-Density Cellulose Rich New Natural Fiber Extracted from the Bark of Jack Tree Branches and Its Characterizations. *Heliyon* **2022**, *8*, e11667. [CrossRef]
40. Durai, P.N.; Viswalingam, K.; Senthilkumar, B.; Divakaran, D.; Siengchin, S. Effect of Alkalization on Physical, Chemical, Thermal, Tensile, and Surface Morphological Properties of Musa Acuminata Peduncles Fiber. *Biomass Convers. Biorefinery* **2023**, *14*, 19753–19764. [CrossRef]
41. Indran, S.; Raj, R.E.; Sreenivasan, V.S. Characterization of New Natural Cellulosic Fiber from Cissus Quadrangularis Root. *Carbohydr. Polym.* **2014**, *110*, 423–429. [CrossRef] [PubMed]
42. Manivel, S.; Pannirselvam, N.; Gopinath, R.; Sathishkumar, T. Physico-Mechanical, Chemical Composition and Thermal Properties of Cellulose Fiber from Hibiscus Vitifolius Plant Stalk for Polymer Composites. *J. Nat. Fibers* **2022**, *19*, 6961–6976. [CrossRef]
43. Indran, S.; Divya, D.; Raja, S.; Sanjay, M.; Siengchin, S. Physico-Chemical, Mechanical and Morphological Characterization of Furcraea Selloa K. *Koch Plant Leaf Fibers-an Exploratory Investigation.* **2023**, *20*, 2146829.
44. Alotaibi, M.D.; Alshammari, B.A.; Saba, N.; Alothman, O.Y.; Sanjay, M.R.; Almutairi, Z.; Jawaid, M. Characterization of Natural Fiber Obtained from Different Parts of Date Palm Tree (*Phoenix dactylifera* L.). *Int. J. Biol. Macromol.* **2019**, *135*, 69–76. [CrossRef] [PubMed]
45. Reddy, K.O.; Ashok, B.; Reddy, K.R.N.; Feng, Y.E.; Zhang, J.; Rajulu, A.V. Extraction and Characterization of Novel Lignocellulosic Fibers from Thespesia Lampas Plant. *Int. J. Polym. Anal. Charact.* **2014**, *19*, 48–61. [CrossRef]

46. Moshi, A.A.M.; Ravindran, D.; Bharathi, S.S.; Indran, S.; Saravanakumar, S.S.; Liu, Y. Characterization of a New Cellulosic Natural Fiber Extracted from the Root of Ficus Religiosa Tree. *Int. J. Biol. Macromol.* **2020**, *142*, 212–221. [CrossRef] [PubMed]
47. Qaiss, A.; Bouhfid, R.; Essabir, H. Effect of Processing Conditions on the Mechanical and Morphological Properties of Composites Reinforced by Natural Fibres. In *Manufacturing of Natural Fibre Reinforced Polymer Composites*; Springer: Cham, Switzerland, 2015; pp. 177–197.
48. Qaiss, A.; Bouhfid, R.; Essabir, H. Characterization and Use of Coir, Almond, Apricot, Argan, Shells, and Wood as Reinforcement in the Polymeric Matrix in Order to Valorize These Products. In *Agricultural Biomass Based Potential Materials*; Springer: Cham, Switzerland, 2015; pp. 305–339.
49. Gopinath, R.; Billigraham, P.; Sathishkumar, T. Physico-Chemical, Mechanical and Thermal Properties of Novel Cellulosic Fiber Extracted from the Bark of Tithonia Diversifolia. *J. Nat. Fibers* **2023**, *20*, 2170944. [CrossRef]
50. De Rosa, I.M.; Kenny, J.M.; Maniruzzaman, M.; Moniruzzaman, M.; Monti, M.; Puglia, D.; Santulli, C.; Sarasini, F. Effect of Chemical Treatments on the Mechanical and Thermal Behaviour of Okra (*Abelmoschus esculentus*) Fibres. *Compos. Sci. Technol.* **2011**, *71*, 246–254. [CrossRef]
51. Rathinavelu, R.; Paramathma, B.S. Examination of Characteristic Features of Raw and Alkali-Treated Cellulosic Plant Fibers from Ventilago Maderaspatana for Composite Reinforcement. *Biomass Convers. Biorefinery* **2023**, *13*, 4413–4425. [CrossRef]
52. Binoj, J.; Raj, R.E.; Indran, S. Characterization of Industrial Discarded Fruit Wastes (*Tamarindus indica* L.) as Potential Alternate for Man-Made Vitreous Fiber in Polymer Composites. *Process Saf. Environ. Prot.* **2018**, *116*, 527–534. [CrossRef]
53. Neto, C.P.; Seca, A.; Fradinho, D.; Coimbra, M.; Domingues, F.; Evtuguin, D.; Silvestre, A.; Cavaleiro, J. Chemical Composition and Structural Features of the Macromolecular Components of Hibiscus Cannabinus Grown in Portugal. *Ind. Crops Prod.* **1996**, *5*, 189–196. [CrossRef]
54. Khan, A.; Vijay, R.; Singaravelu, D.L.; Sanjay, M.R.; Siengchin, S.; Jawaid, M.; Alamry, K.A.; Asiri, A.M. Extraction and Characterization of Natural Fibers from Citrullus Lanatus Climber. *J. Nat. Fibers* **2022**, *19*, 621–629. [CrossRef]
55. Kumar, R.; Hynes, N.R.J.; Senthamaraikannan, P.; Saravanakumar, S.; Sanjay, M.R. Physicochemical and Thermal Properties of Ceiba Pentandra Bark Fiber. *J. Nat. Fibers* **2018**, *15*, 822–829. [CrossRef]
56. Chanzy, H.; Imada, K.; Mollard, A.; Vuong, R.; Barnoud, F. Crystallographic Aspects of Sub-Elementary Cellulose Fibrils Occurring in the Wall of Rose Cells Cultured in Vitro. *Protoplasma* **1979**, *100*, 303–316. [CrossRef]
57. Madhu, P.; Sanjay, M.; Pradeep, S.; Bhat, K.S.; Yogesha, B.; Siengchin, S. Characterization of Cellulosic Fibre from Phoenix Pusilla Leaves as Potential Reinforcement for Polymeric Composites. *J. Mater. Res. Technol.* **2019**, *8*, 2597–2604. [CrossRef]
58. Ahmed, J.; Balaji, M.A.; Saravanakumar, S.S.; Senthamaraikannan, P. A Comprehensive Physical, Chemical and Morphological Characterization of Novel Cellulosic Fiber Extracted from the Stem of Elettaria Cardamomum Plant. *J. Nat. Fibers* **2021**, *18*, 1460–1471. [CrossRef]
59. Manimaran, P.; Saravanan, S.P.; Sanjay, M.R.; Siengchin, S.; Jawaid, M.; Khan, A. Characterization of New Cellulosic Fiber: Dracaena Reflexa as a Reinforcement for Polymer Composite Structures. *J. Mater. Res. Technol.* **2019**, *8*, 1952–1963. [CrossRef]
60. Kar, A.; Saikia, D.; Palanisamy, S.; Santulli, C.; Fragassa, C.; Thomas, S. Effect of Alkali Treatment under Ambient and Heated Conditions on the Physicochemical, Structural, Morphological, and Thermal Properties of Calamus Tenuis Cane Fibers. *Fibers* **2023**, *11*, 92. [CrossRef]
61. Pokhriyal, M.; Rakesh, P.K.; Rangappa, S.M.; Siengchin, S. Effect of Alkali Treatment on Novel Natural Fiber Extracted from *Himalayacalamus falconeri* Culms for Polymer Composite Applications. *Biomass Convers. Biorefinery* **2023**, *14*, 18481–18497. [CrossRef]
62. Palaniappan, M.; Palanisamy, S.; Murugesan, T.M.; Alrasheedi, N.H.; Ataya, S.; Tadepalli, S.; Elfar, A.A. Novel *Ficus retusa* L. Aerial Root Fiber: A Sustainable Alternative for Synthetic Fibres in Polymer Composites Reinforcement. *Biomass Convers. Biorefinery* **2024**, 1–17. [CrossRef]
63. Monteiro, S.N.; Calado, V.; Rodriguez, R.J.S.; Margem, F.M. Thermogravimetric Behavior of Natural Fibers Reinforced Polymer Composites—An Overview. *Mater. Sci. Eng. A* **2012**, *557*, 17–28. [CrossRef]
64. Abebaw, N.; Baye, B. Extraction and Characterization of Hibiscus Macrantus Bast Fibers as a Reinforcement Material for Composite Application. *Polym. Bull.* **2023**, *80*, 7407–7427. [CrossRef]
65. Paajanen, A.; Rinta-Paavola, A.; Vaari, J. High-Temperature Decomposition of Amorphous and Crystalline Cellulose: Reactive Molecular Simulations. *Cellulose* **2021**, *28*, 8987–9005. [CrossRef]
66. Sahayaraj, A.F.; Selvan, M.T.; Ramesh, M.; Maniraj, J.; Jenish, I.; Nagarajan, K. Extraction, Purification, and Characterization of Novel Plant Fiber from Tabernaemontana Divaricate Stem to Use as Reinforcement in Polymer Composites. *Biomass Convers. Biorefinery* **2024**, 1–15. [CrossRef]
67. Vinod, A.; Vijay, R.; Lenin Singaravelu, D.; Khan, A.; Sanjay, M.; Siengchin, S.; Verpoort, F.; Alamry, K.A.; Asiri, A.M. Effect of Alkali Treatment on Performance Characterization of Ziziphus Mauritiana Fiber and Its Epoxy Composites. *J. Ind. Text.* **2022**, *51*, 2444S–2466S. [CrossRef]

68. Senthamaraikannan, P.; Saravanakumar, S. Evaluation of Characteristic Features of Untreated and Alkali-Treated Cellulosic Plant Fibers from Mucuna Atropurpurea for Polymer Composite Reinforcement. *Biomass Convers. Biorefinery* **2023**, *13*, 11295–11309. [CrossRef]
69. Keskin, O.Y.; Koktas, S.; Seki, Y.; Dalmis, R.; Kilic, G.B.; Albayrak, D. Natural Cellulosic Fiber from Carex Panicea Stem for Polymer Composites: Extraction and Characterization. *Biomass Convers. Biorefinery* **2024**, *14*, 13901–13912. [CrossRef]
70. Ilangovan, M.; Guna, V.; Prajwal, B.; Jiang, Q.; Reddy, N. Extraction and Characterisation of Natural Cellulose Fibers from Kigelia Africana. *Carbohydr. Polym.* **2020**, *236*, 115996. [CrossRef] [PubMed]
71. Senthilraja, R.; Sarala, R.; Manimaran, P. Characterization of New Natural Cellulosic Fiber from the Bark of Artocarpus Altilis Plant. *J. Nat. Fibers* **2023**, *20*, 2150923.
72. Balachandran, G.B.; Narayanasamy, P.; Alexander, A.B.; David, P.W.; Mariappan, R.K.; Ramachandran, M.E.; Indran, S.; Rangappa, S.M.; Siengchin, S. Multi-Analytical Investigation of the Physical, Chemical, Morphological, Tensile, and Structural Properties of Indian Mulberry (*Morinda tinctoria*) Bark Fibers. *Heliyon* **2023**, *9*, e21239. [CrossRef]
73. Drouiche, F.; Laouici, H.; Cheikh, M. Morphological, Chemical, Thermal and Mechanical Analysis of Doum Fibers as Potential Reinforcement of Polymer Composites. *J. Compos. Mater.* **2024**, *58*, 37–54. [CrossRef]
74. Rahman, M.F.; Wu, J.; Tseng, T.L.B. Automatic Morphological Extraction of Fibers from SEM Images for Quality Control of Short Fiber-Reinforced Composites Manufacturing. *CIRP J. Manuf. Sci. Technol.* **2021**, *33*, 176–187. [CrossRef]
75. Purushothaman, R.; Balaji, A.; Swaminathan, J. Influence of NaOH Treatment on Physical, Chemical, Thermal, and Morphological Behavior of Aloe Vera, Banana, and Corn Husk Fiber. *Biomass Convers. Biorefinery* **2024**, *14*, 16743–16754. [CrossRef]
76. Hindi, J.; Abdul Salam, A.A.; K, M.; BM, G.; YM, S.; Ibrahim, A. Characterization of Novel Cellulosic Salvadora Persica Fiber for Potentiality in Polymer Matrix Composites. *J. Nat. Fibers* **2024**, *21*, 2409874. [CrossRef]
77. Raja, T.; Devarajan, Y. Effective Utilization of Fibre Extracted from the Waste Neem Tree Twigs—A Step towards Sustainable Practices. *Biomass Convers. Biorefinery* **2023**, *14*, 21049–21057. [CrossRef]
78. Selvaraj, S.K.; Saravanan, K. Characterization and Potential Applications of Grewia Hirsuta Fibers: Nature's Own Composite Materials. *Biomass Convers. Biorefinery* **2024**, 1–9. [CrossRef]
79. Maran, M.; Kumar, R.; Senthamaraikannan, P.; Saravanakumar, S.; Nagarajan, S.; Sanjay, M.; Siengchin, S. Suitability Evaluation of Sida Mysorensis Plant Fiber as Reinforcement in Polymer Composite. *J. Nat. Fibers* **2022**, *19*, 1659–1669. [CrossRef]
80. Wrzecionek, M.; Matyszczak, G.; Bandzerewicz, A.; Ruśkowski, P.; Gadomska-Gajadhur, A. Kinetics of Polycondensation of Citric Acid with Glycerol Based on a Genetic Algorithm. *Org. Process Res. Dev.* **2021**, *25*, 271–281. [CrossRef]
81. Tisserat, B.; O'kuru, R.H.; Hwang, H.; Mohamed, A.A.; Holser, R. Glycerol Citrate Polyesters Produced through Heating without Catalysis. *J. Appl. Polym. Sci.* **2012**, *125*, 3429–3437. [CrossRef]
82. Berube, M.-A.; Schorr, D.; Ball, R.J.; Landry, V.; Blanchet, P. Determination of in Situ Esterification Parameters of Citric Acid-Glycerol Based Polymers for Wood Impregnation. *J. Polym. Environ.* **2018**, *26*, 970–979. [CrossRef]
83. Hassan, T.; Jamshaid, H.; Mishra, R.; Khan, M.Q.; Petru, M.; Novak, J.; Choteborsky, R.; Hromasova, M. Acoustic, Mechanical and Thermal Properties of Green Composites Reinforced with Natural Fibers Waste. *Polymers* **2020**, *12*, 654. [CrossRef] [PubMed]
84. Shakir, M.A.; Ahmad, M.I.; Yusup, Y.; Wabaidur, S.M.; Siddiqui, M.R.; Alam, M.; Rafatullah, M. Sandwich Composite Panel from Spent Mushroom Substrate Fiber and Empty Fruit Bunch Fiber for Potential Green Thermal Insulation. *Buildings* **2023**, *13*, 224. [CrossRef]
85. Sinha, A.K.; Narang, H.K.; Bhattacharya, S. Mechanical Properties of Natural Fibre Polymer Composites. *J. Polym. Eng.* **2017**, *37*, 879–895. [CrossRef]
86. Tůmová, E.; Drochytka, R.; Černý, V.; Čada, P. Development of Organic and Biodegradable Insulating Material for ETICS. *Procedia Eng.* **2017**, *195*, 81–87. [CrossRef]
87. Khalaf, Y.; El Hage, P.; Mihajlova, J.D.; Bergeret, A.; Lacroix, P.; El Hage, R. Influence of Agricultural Fibers Size on Mechanical and Insulating Properties of Innovative Chitosan-Based Insulators. *Constr. Build. Mater.* **2021**, *287*, 123071. [CrossRef]
88. Bakatovich, A.; Davydenko, N.; Gaspar, F. Thermal Insulating Plates Produced on the Basis of Vegetable Agricultural Waste. *Energy Build.* **2018**, *180*, 72–82. [CrossRef]
89. Tigabe, S.; Atalie, D.; Gideon, R.K. Physical Properties Characterization of Polyvinyl Acetate Composite Reinforced with Jute Fibers Filled with Rice Husk and Sawdust. *J. Nat. Fibers* **2022**, *19*, 5928–5939. [CrossRef]
90. Jaber, A.A.; Abbas, S.A.; Farah, A.A.; Kopeć, K.K.; Alsalik, Y.M.; Tayeb, M.A.; Verghese, N. Effect of Fiber Sizing Levels on the Mechanical Properties of Carbon Fiber-Reinforced Thermoset Composites. *Polymers* **2023**, *15*, 4678. [CrossRef] [PubMed]
91. Pakravan, H.; Latifi, M.; Jamshidi, M. Hybrid Short Fiber Reinforcement System in Concrete: A Review. *Constr. Build. Mater.* **2017**, *142*, 280–294. [CrossRef]
92. Mills, P.; Seville, J.; Knight, P.; Adams, M. The Effect of Binder Viscosity on Particle Agglomeration in a Low Shear Mixer/Agglomerator. *Powder Technol.* **2000**, *113*, 140–147. [CrossRef]
93. Bouraima, M.B.; Zhang, X.; Zhou, S.; Qiu, Y. Impact of Viscosity Modifier on Asphalt Properties Used for Bus Rapid Transit Lane in Chengdu. *J. Mod. Transp.* **2017**, *25*, 185–193. [CrossRef]

94. Keningley, S.; Knight, P.; Marson, A. An Investigation into the Effects of Binder Viscosity on Agglomeration Behaviour. *Powder Technol.* **1997**, *91*, 95–103. [CrossRef]
95. Paiva, A.; Pereira, S.; Sá, A.; Cruz, D.; Varum, H.; Pinto, J. A Contribution to the Thermal Insulation Performance Characterization of Corn Cob Particleboards. *Energy Build.* **2012**, *45*, 274–279. [CrossRef]
96. Abdou, A.; Budaiwi, I. The Variation of Thermal Conductivity of Fibrous Insulation Materials under Different Levels of Moisture Content. *Constr. Build. Mater.* **2013**, *43*, 533–544. [CrossRef]
97. Elfordy, S.; Lucas, F.; Tancret, F.; Scudeller, Y.; Goudet, L. Mechanical and Thermal Properties of Lime and Hemp Concrete ("Hempcrete") Manufactured by a Projection Process. *Constr. Build. Mater.* **2008**, *22*, 2116–2123. [CrossRef]
98. Xu, J.; Sugawara, R.; Widyorini, R.; Han, G.; Kawai, S. Manufacture and Properties of Low-Density Binderless Particleboard from Kenaf Core. *J. Wood Sci.* **2004**, *50*, 62–67. [CrossRef]
99. Salas-Ruiz, A.; del Mar Barbero-Barrera, M.; Ruiz-Téllez, T. Microstructural and Thermo-Physical Characterization of a Water Hyacinth Petiole for Thermal Insulation Particle Board Manufacture. *Materials* **2019**, *12*, 560. [CrossRef]
100. Cintura, E.; Faria, P.; Molari, L.; Barbaresi, L.; D'Orazio, D.; Nunes, L. Characterization of an Arundo Donax-Based Composite: A Solution to Improve Indoor Comfort. *Ind. Crops Prod.* **2024**, *208*, 117756. [CrossRef]
101. Cintura, E.; Nunes, L.; Molari, L.; Bettuzzi, M.; Morigi, M.P.; Brancaccio, R.; Faria, P. Hygroscopicity and Morphology of Bio-Based Boards—The Influence of the Formulation. *Appl. Sci.* **2024**, *14*, 873. [CrossRef]
102. Cintura, E.; Faria, P.; Molari, L.; Barbaresi, L.; D'Orazio, D.; Nunes, L. A Feasible Re-Use of an Agro-Industrial by-Product: Hazelnut Shells as High-Mass Bio-Aggregate in Boards for Indoor Applications. *J. Clean. Prod.* **2024**, *434*, 140297. [CrossRef]
103. Ferrandez-Villena, M.; Ferrandez-Garcia, C.E.; Garcia-Ortuño, T.; Ferrandez-Garcia, A.; Ferrandez-Garcia, M.T. Analysis of the Thermal Insulation and Fire-Resistance Capacity of Particleboards Made from Vine (*Vitis vinifera* L.) Prunings. *Polymers* **2020**, *12*, 1147. [CrossRef] [PubMed]
104. Ninikas, K.; Mitani, A.; Koutsianitis, D.; Ntalos, G.; Taghiyari, H.R.; Papadopoulos, A.N. Thermal and Mechanical Properties of Green Insulation Composites Made from Cannabis and Bark Residues. *J. Compos. Sci.* **2021**, *5*, 132. [CrossRef]
105. Terekhov, I.V.; Chistyakov, E.M. Binders Used for the Manufacturing of Composite Materials by Liquid Composite Molding. *Polymers* **2021**, *14*, 87. [CrossRef]
106. Zhou, Y.; Trabelsi, A.; El Mankibi, M. Development and Characterization of Thermal Insulation Materials Based on Rice Straw and Natural Binder. In Proceedings of the 2022: CLIMA 2022 The 14th REHVA HVAC World Congress, Rotterdam, The Netherlands, 22–25 May 2022.
107. Chikhi, M.; Agoudjil, B.; Boudenne, A.; Gherabli, A. Experimental Investigation of New Biocomposite with Low Cost for Thermal Insulation. *Energy Build.* **2013**, *66*, 267–273. [CrossRef]
108. Evon, P.; Vandenbossche, V.; Pontalier, P.-Y.; Rigal, L. New Thermal Insulation Fiberboards from Cake Generated during Biorefinery of Sunflower Whole Plant in a Twin-Screw Extruder. *Ind. Crops Prod.* **2014**, *52*, 354–362. [CrossRef]
109. Mati-Baouche, N.; De Baynast, H.; Lebert, A.; Sun, S.; Lopez-Mingo, C.J.S.; Leclaire, P.; Michaud, P. Mechanical, Thermal and Acoustical Characterizations of an Insulating Bio-Based Composite Made from Sunflower Stalks Particles and Chitosan. *Ind. Crops Prod.* **2014**, *58*, 244–250. [CrossRef]
110. Bakatovich, A.; Gaspar, F. Composite Material for Thermal Insulation Based on Moss Raw Material. *Constr. Build. Mater.* **2019**, *228*, 116699. [CrossRef]
111. Liu, Z.; Lei, Y.; Zhang, X.; Kang, Z.; Zhang, J. Effect Mechanism and Simulation of Voids on Hygrothermal Performances of Composites. *Polymers* **2022**, *14*, 901. [CrossRef] [PubMed]
112. Mehdikhani, M.; Gorbatikh, L.; Verpoest, I.; Lomov, S.V. Voids in Fiber-Reinforced Polymer Composites: A Review on Their Formation, Characteristics, and Effects on Mechanical Performance. *J. Compos. Mater.* **2019**, *53*, 1579–1669. [CrossRef]
113. Selamat, M.Z.; Tahir, M.S.Z.; Kasim, A.N.; Dharmalingam, S.; Putra, A.; Yaakob, M.Y.; Daud, M.A.M. Effect of Starch Sizes Particle as Binder on Short Pineapple Leaf Fiber Composite Mechanical Properties. *EDP Sci.* **2018**, *150*, 04008. [CrossRef]
114. Pundiene, I.; Vitola, L.; Pranckeviciene, J.; Bajare, D. Hemp Shive-Based Bio-Composites Bounded by Potato Starch Binder: The Roles of Aggregate Particle Size and Aspect Ratio. *J. Ecol. Eng.* **2022**, *23*, 220–234. [CrossRef] [PubMed]
115. Frantz, N.; Dutra, L.F.; Nguyen, D.M.; Almeida, G.; Perré, P. Effects of Phase Ratios, Density and Particle Shapes on Directional Thermal Conductivity of Vegetable Concrete: A Predictive Model. *Constr. Build. Mater.* **2024**, *410*, 134238. [CrossRef]
116. Chen, S.; Fan, H.; Su, Y.; Li, W.; Li, J.; Yan, B.; Song, J.; Hu, L.; Zhang, Y. Influence of Binder Systems on Sintering Characteristics, Microstructures, and Mechanical Properties of PcBN Composites Fabricated by SPS. *J. Adv. Ceram.* **2022**, *11*, 321–330. [CrossRef]

117. Zannen, S.; Ghali, L.; Halimi, M.T.; Hssen, M.B. Effect of Chemical Extraction on Physicochemical and Mechanical Properties of Doum Palm Fibres. *Adv. Mater. Phys. Chem.* **2014**, *04*, 203–216. [CrossRef]
118. Unterweger, C.; Brüggemann, O.; Fürst, C. Effects of Different Fibers on the Properties of Short-Fiber-Reinforced Polypropylene Composites. *Compos. Sci. Technol.* **2014**, *103*, 49–55. [CrossRef]